– Supporting Information –

Alkali element (Li, Na, K, and Rb) doping of $Cu_2BaGe_{1-x}Sn_xSe_4$ films

Yongshin Kim,[1] Hannes Hempel,[2] Steven P. Harvey,[3] Nelson A. Rivera,[4] Thomas Unold,[2] David B. Mitzi[1,5]*

[1]Department of Mechanical Engineering and Materials Science, Duke University, Durham, North Carolina 27708, USA.

[2]Department Structure and Dynamics of Energy Materials, Helmholtz-Zentrum Berlin für Materialien und Energie GmbH, Hahn-Meitner-Platz 1, 14109, Berlin, Germany

[3]Renewable and Sustainable Energy Institute, University of Colorado Boulder, Boulder Colorado 80309 USA

[4]Department of Civil and Environmental Engineering, Duke University, Durham, North Carolina 27708, USA.

[5]Department of Chemistry, Duke University, Durham, North Carolina 27708, USA.
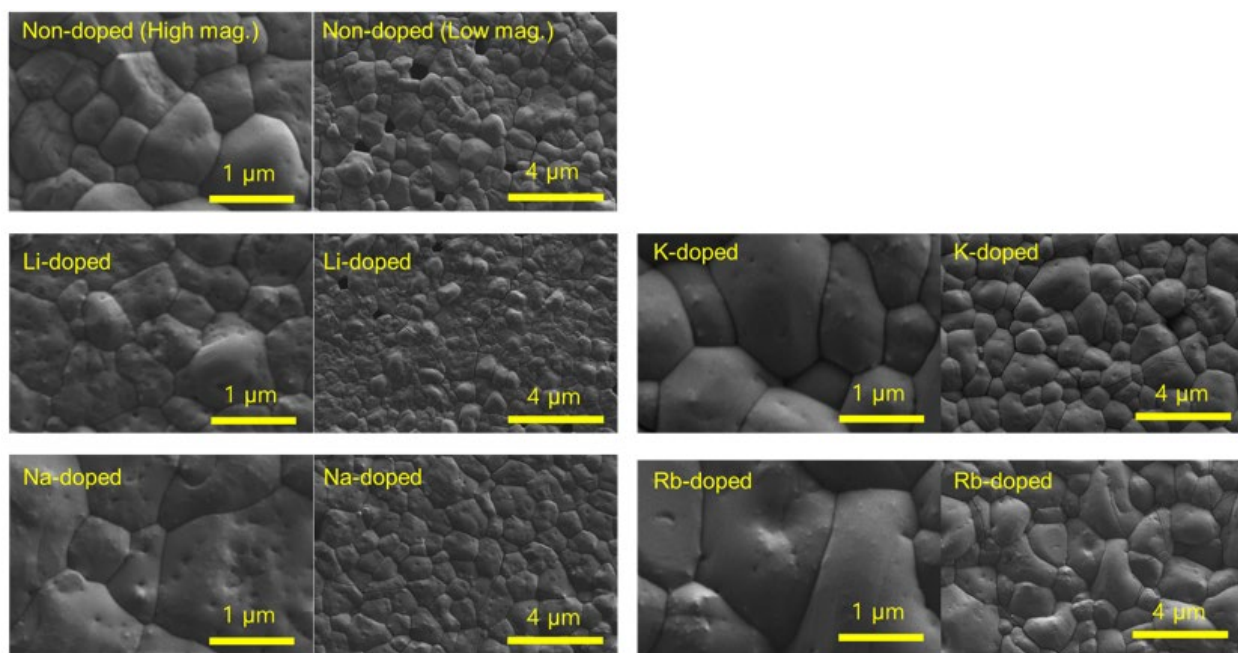
E-mail: david.mitzi@duke.edu

Fig. S1 High magnification (1 μm scale bar) and low magnification (4 μm scale bar) SEM surface images (2 kV acceleration voltage) of non-doped and alkali-doped CBGTSe films deposited on quartz glass substrates. For alkali-doped films, 4 nm of LiF, NaF, KF, and RbF layers were pre-deposited prior to deposition of CBGTSe. The average grain sizes (square root of the area divided by number of grains) determined from the low magnification images were ~0.84 μm for undoped, ~0.78 μm for Li-doped, ~1.08 μm for Na-doped, ~1.15 μm for K-doped, and ~1.35 μm for Rb-doped films.
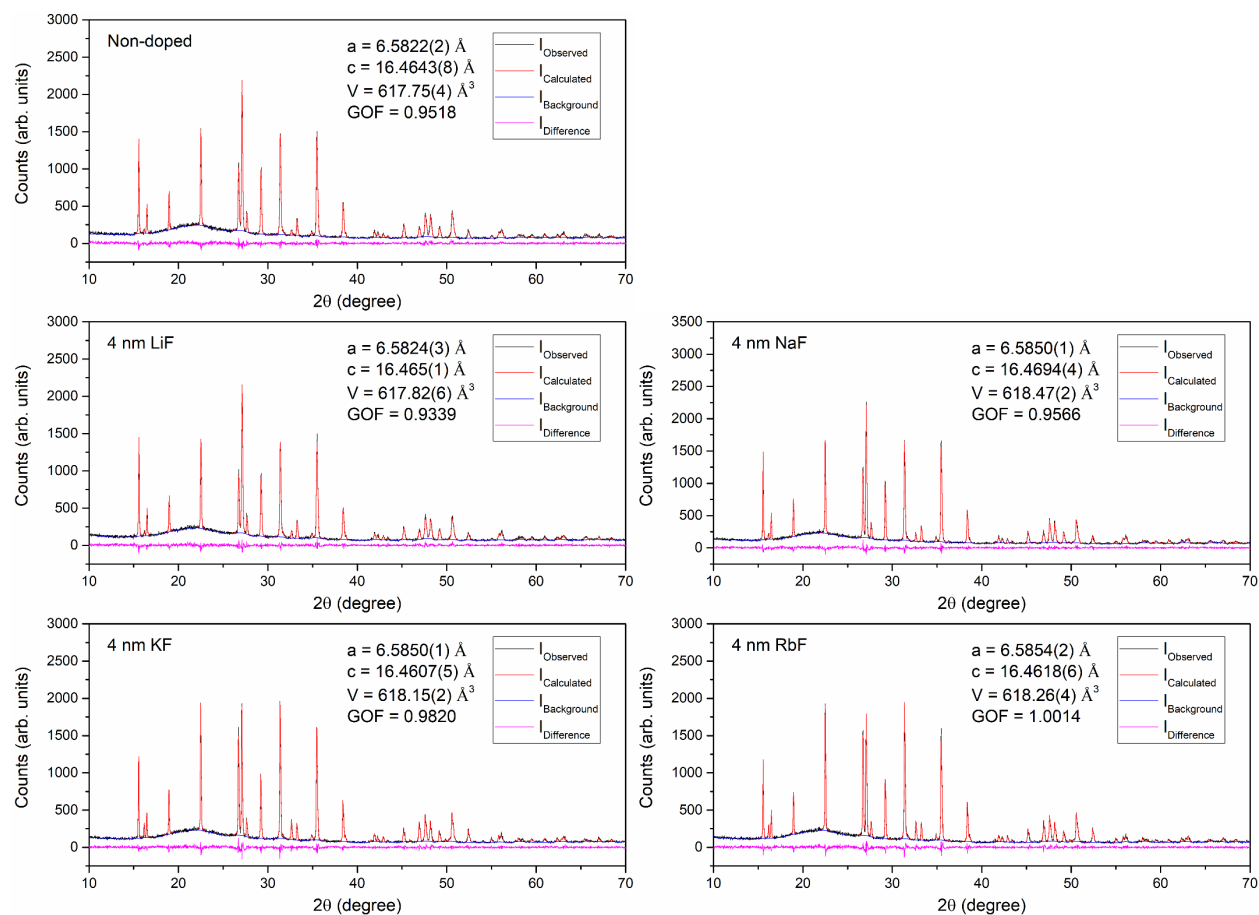
Fig. S2 Pawley phase fitting results for non-doped and alkali-doped CBGTSe films prepared with pre-deposition of 4 nm alkali fluoride layers on quartz glass substrates (no pre-deposition for non-doped sample). Signals from the quartz glass substrates were set as background. Lattice constants (*a, c*), lattice volume (*V*), and goodness of fit (GOF) derived from the Pawley fits are also summarized in the figure.
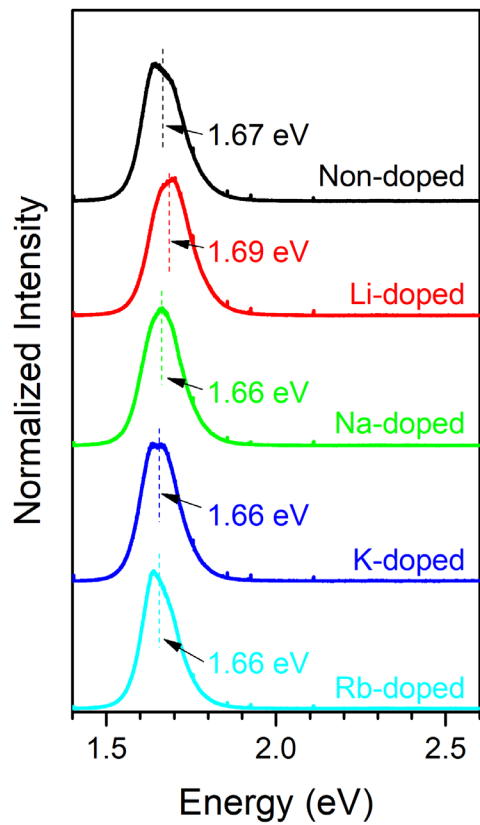
Fig. S3 Photoluminescence (PL) spectra for the non-doped and alkali-doped CBGTSe films prepared with pre-deposition of 4 nm alkali fluoride layers (no pre-deposition for non-doped sample).
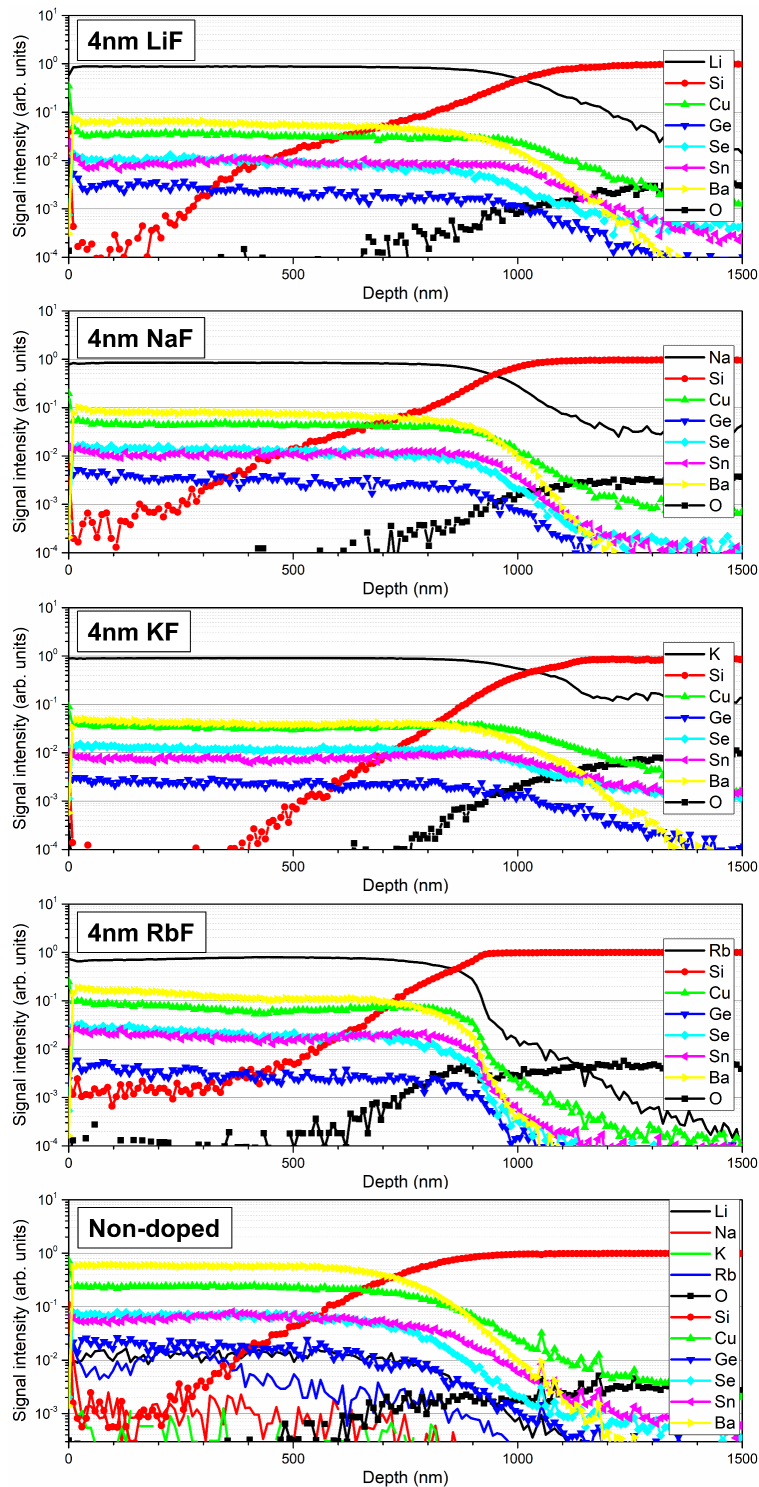
Fig. S4 TOF-SIMS elemental depth profile for non-doped and alkali-doped CBGTSe films prepared with pre-deposition of 4-nm-thick alkali fluoride layers on quartz glass substrates (no pre-deposition for non-doped sample). Each elemental signal is normalized to the total signal.
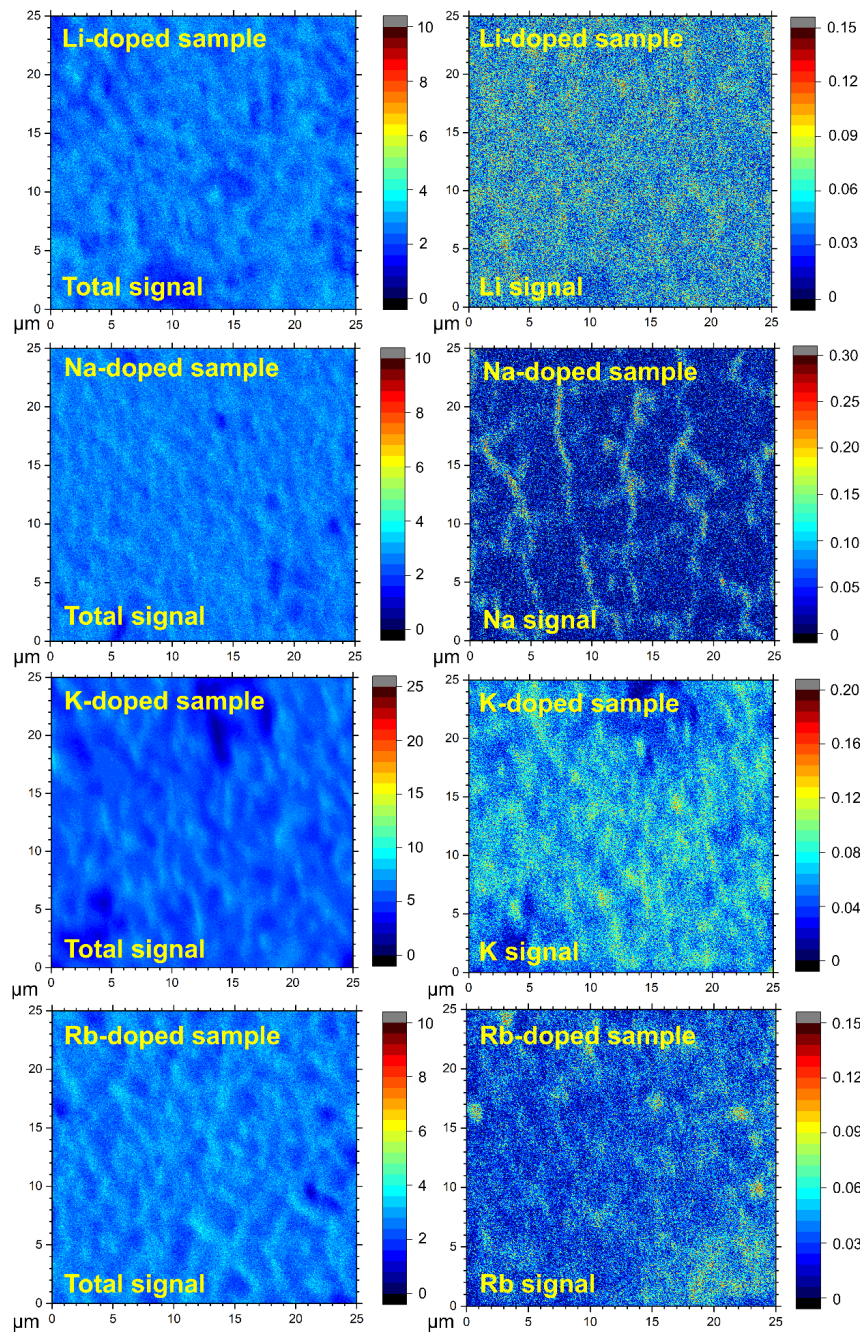
Fig. S5 TOF-SIMS 2D images for alkali-doped CBGTSe films prepared with pre-deposition of 4 nm alkali fluoride layers showing (left) total signal counts and (right) alkali-element signals. Each image was obtained by integrating the signals over 0.2–0.6 μm film depth. Because alkali-element signals are not normalized, the alkali-element distribution images may contain influences from film roughness. Each image is 25 μm × 25 μm and the color scale shows the intensity of the signal per pixel (arb. units).
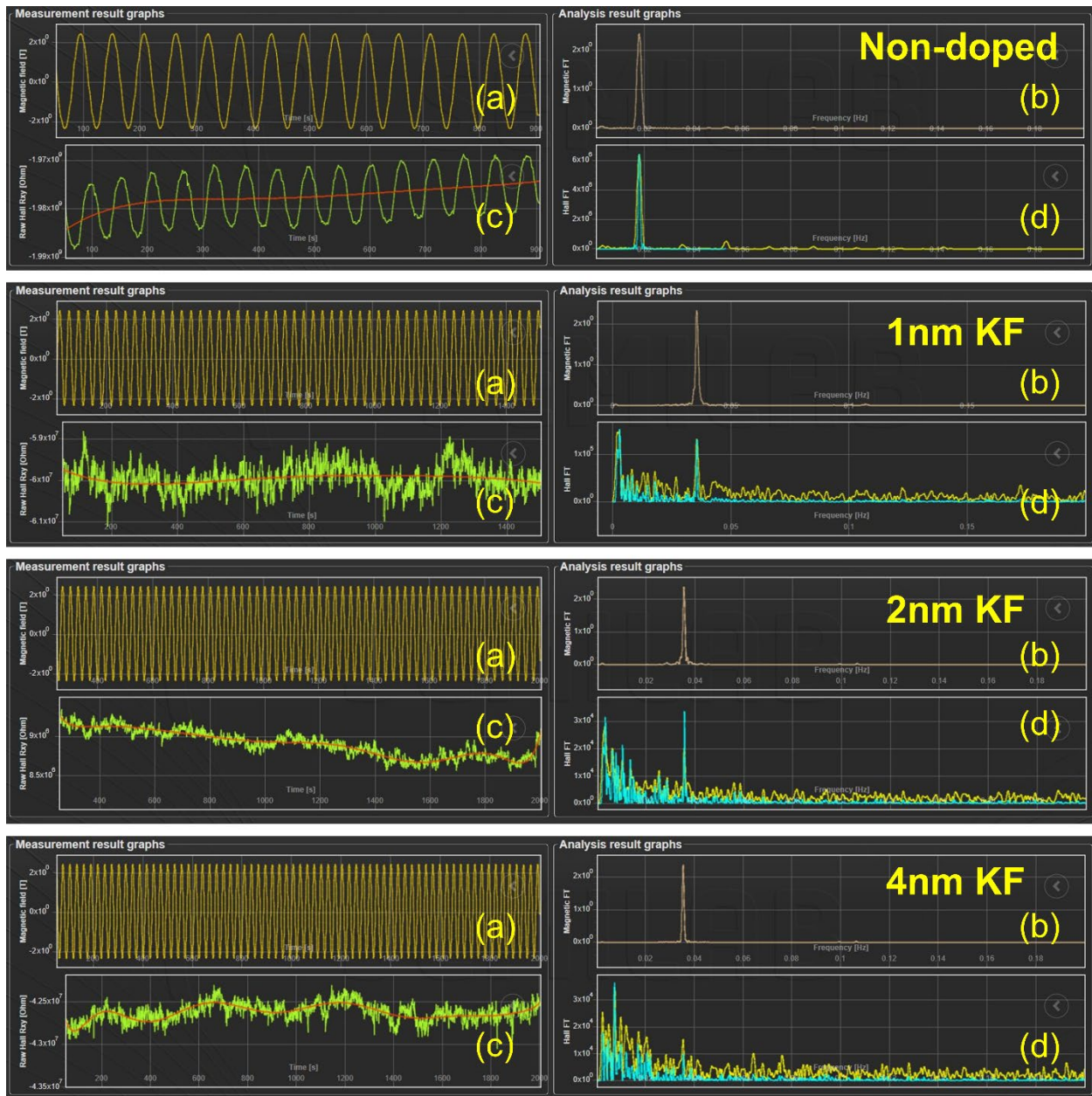
Fig. S6 Hall effect analysis results for non-doped/K-doped CBGTSe samples (*i.e.*, films prepared with pre-deposition of 0 nm, 1 nm, 2 nm, and 4 nm KF layers) using a parallel dipole line (PDL) setup: (a) Magnetic field trace as the reference signal, and (b) Fourier transform of the reference signal. (c) Transverse Hall signal R_{XY}, and (d) Fourier transform of R_{XY}. In (d), the cyan curve is the power spectral density (PSD), and the yellow curve is the Fourier spectrum of the signal. Signals from the doped samples were measured and averaged over longer time (1500–2000 s) than non-doped samples (~900 s) due to their weaker signal levels, arising from the higher carrier density and lower carrier mobility values.
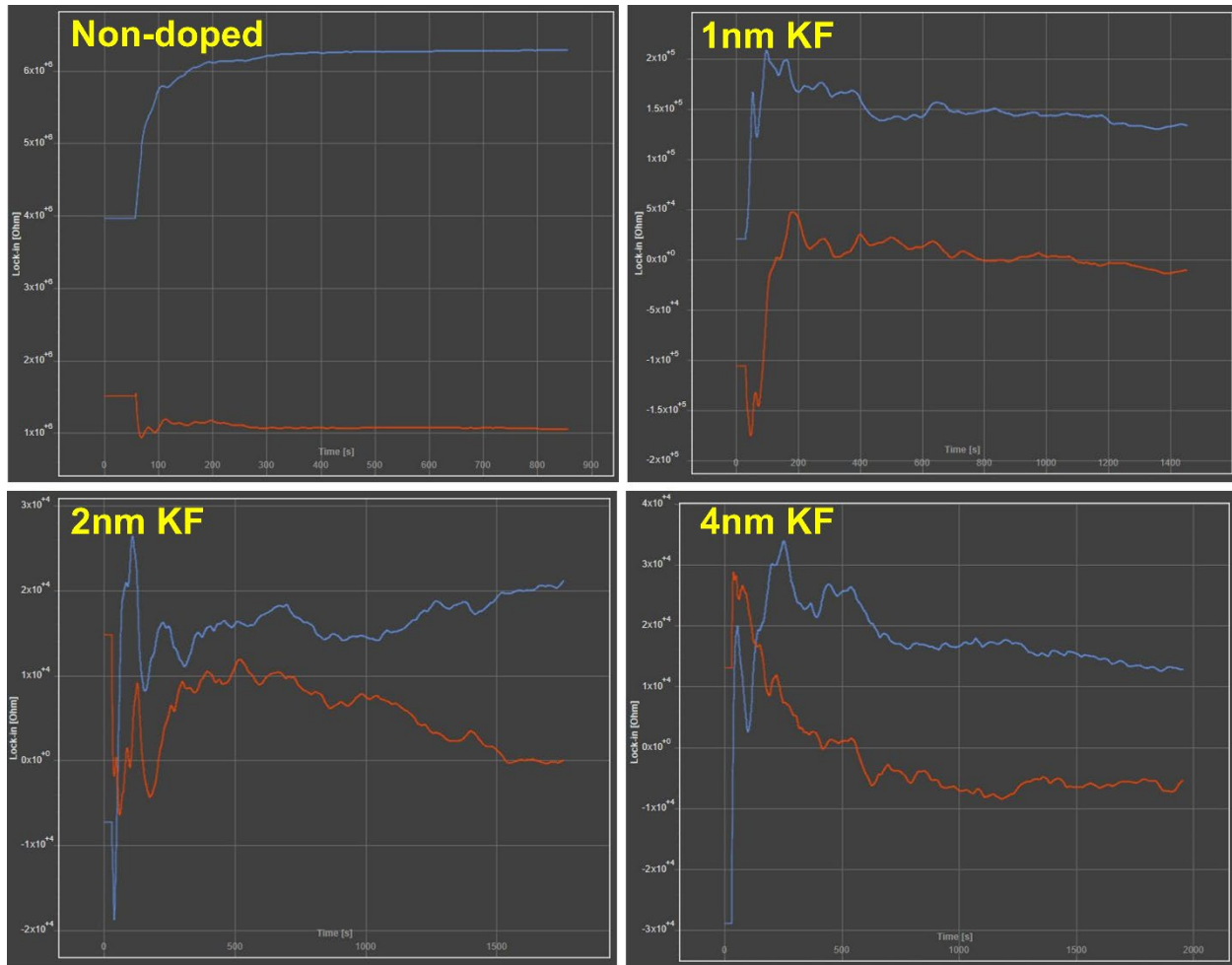
Fig. S7 Hall effect analysis results for non-doped/K-doped CBGTSe samples (*i.e.*, films pre-deposited with 0, 1, 2, and 4 nm KF layers) using a parallel dipole line (PDL) setup: Lock-in detection of the in-phase (Hall signal; blue curve) and out-of-phase (red curve) signals over the time wherein the Hall resistance R_H is extracted. A lock-in time constant of 60 s is used in these examples.
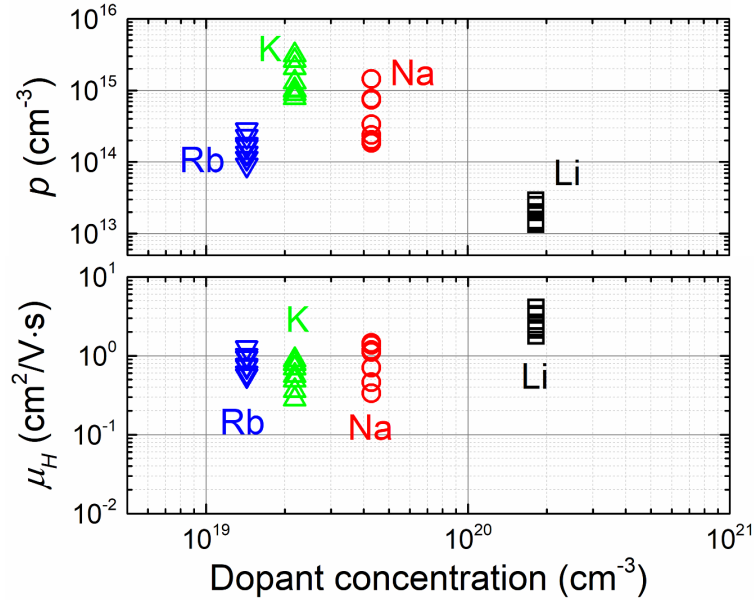
Fig. S8 Hole carrier density (*p*) and Hall mobility (μ_H) plots summarizing data points from CBGTSe films prepared with pre-deposition of 4 nm alkali fluoride layers, as a function of dopant concentrations determined from ICP-MS measurements (**Table 1**).
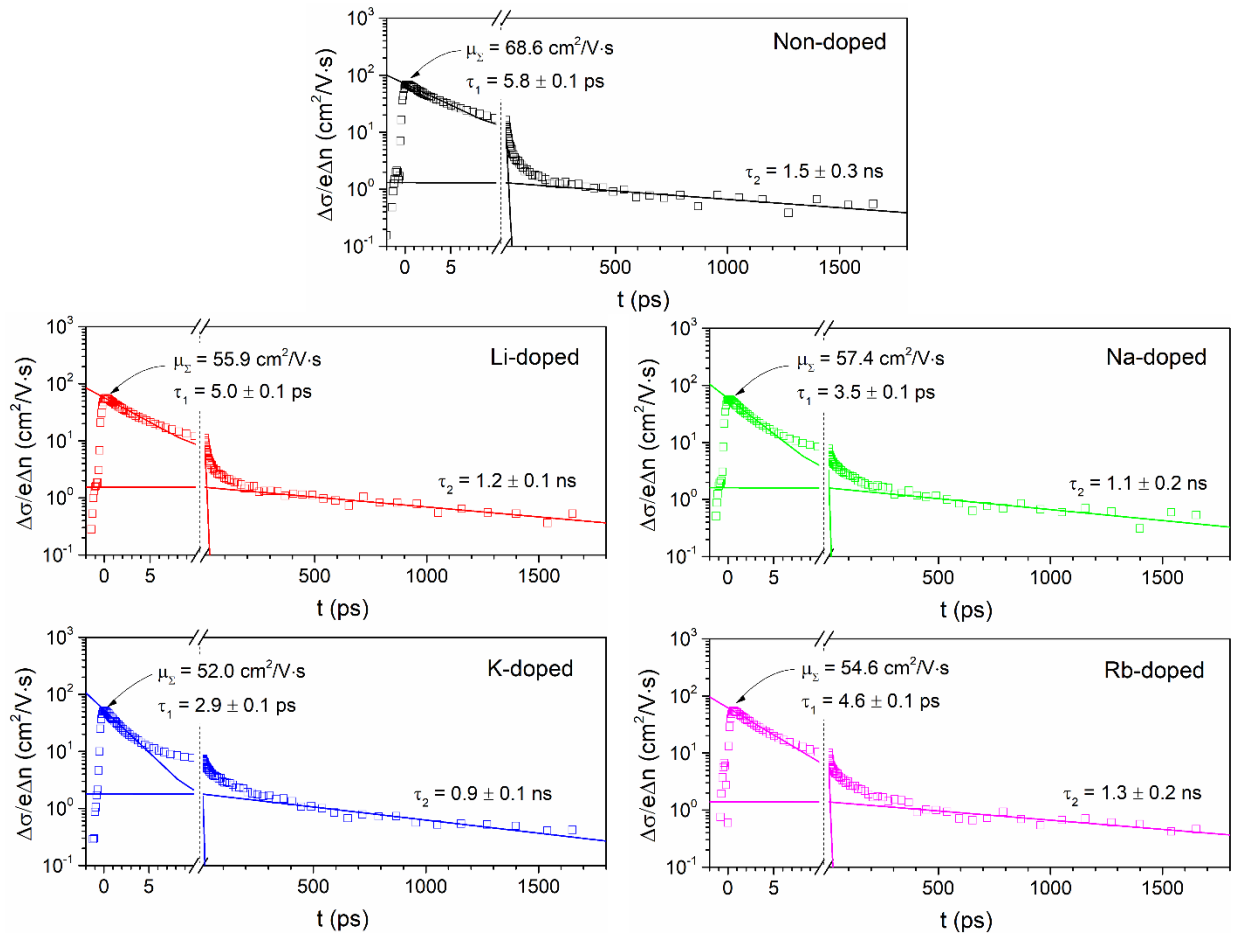
Fig. S9 Exponential decay fitting for fast and slow decay components shown in **Fig. 6**. Solid curves are derived from exponential decay curve fitting to derive decay time constants (τ_1 and τ_2) for fast and slow decay components. Terahertz sum mobility (μ_Σ) values for each sample are also noted.

Table S1 Average Hall measurement parameters (p and μ_H) derived from multiple (8–13) distinct non-doped/alkali-doped CBGTSe films. The errors listed correspond to the standard deviations for each sample type.

Sample		p (cm^{-3})	μ_H (cm^2/V·s)	Sample		p (cm^{-3})	μ_H (cm^2/V·s)
LiF	1nm	$(6.05 \pm 0.89) \times 10^{12}$	3.23 ± 1.04	NaF	1nm	$(7.80 \pm 2.58) \times 10^{13}$	1.93 ± 0.66
	2nm	$(9.38 \pm 2.91) \times 10^{12}$	3.55 ± 1.35		2nm	$(1.76 \pm 1.06) \times 10^{14}$	1.62 ± 0.40
	4nm	$(2.02 \pm 0.58) \times 10^{13}$	2.70 ± 0.79		4nm	$(5.11 \pm 4.46) \times 10^{14}$	0.98 ± 0.42
KF	1nm	$(7.66 \pm 3.10) \times 10^{13}$	1.40 ± 0.44	RbF	1nm	$(1.35 \pm 0.33) \times 10^{13}$	2.23 ± 0.75
	2nm	$(4.44 \pm 2.04) \times 10^{14}$	0.83 ± 0.30		2nm	$(2.74 \pm 1.29) \times 10^{13}$	1.37 ± 0.49
	4nm	$(1.60 \pm 0.88) \times 10^{15}$	0.61 ± 0.22		4nm	$(1.70 \pm 0.62) \times 10^{14}$	0.81 ± 0.25
Non-doped		$(2.22 \pm 0.89) \times 10^{12}$	3.62 ± 0.84				